Journal of Experimental Nanoscience
Publication details, including instructions for authors and subscription information:
http://www.informaworld.com/smpp/title~content=t716100757

Preparation and spectral analysis of Pr^{3+}-doped $BaO-SiO_2$ glass-ceramics

Chenxia Li[ab]; Shiqing Xu[a]; Puyang Zhang[a]; Shilong Zhao[a]; Degang Deng[a]; Songlin Zhuang[b]
[a] College of Optical and Electronic Technology, China Jiliang University, Hangzhou 310018, China [b] Optical and Electronic Information Engineering College, University of Shanghai for Science and Technology, Shanghai 200093, China

Online publication date: 24 March 2010

To cite this Article Li, Chenxia , Xu, Shiqing , Zhang, Puyang , Zhao, Shilong , Deng, Degang and Zhuang, Songlin(2010) 'Preparation and spectral analysis of Pr^{3+}-doped $BaO-SiO_2$ glass-ceramics', Journal of Experimental Nanoscience, 5: 2, 154 — 161
To link to this Article: DOI: 10.1080/17458080903383308
URL: http://dx.doi.org/10.1080/17458080903383308

Journal of Experimental Nanoscience
Vol. 5, No. 2, April 2010, 154–161

Taylor & Francis
Taylor & Francis Group

Preparation and spectral analysis of Pr^{3+}-doped $BaO–SiO_2$ glass-ceramics

Chenxia Li[ab], Shiqing Xu[a]*, Puyang Zhang[a], Shilong Zhao[a], Degang Deng[a] and Songlin Zhuang[b]

[a]*College of Optical and Electronic Technology, China Jiliang University, Hangzhou 310018, China;* [b]*Optical and Electronic Information Engineering College, University of Shanghai for Science and Technology, Shanghai 200093, China*

(*Received 10 June 2009; final version received 2 October 2009*)

A study of the optical properties of Pr^{3+} ions in oxy glass and glass ceramics (GCs) was carried out. X-ray diffraction (XRD), Raman, excitation and emission spectra of GCs were measured. XRD and Raman spectrum confirmed the formation of β-$BaSiO_3$ nanocrystals in the glassy matrix. The emission luminescence intensity of Pr^{3+} ions in the GCs increased significantly with increasing crystallisation temperature and the reasons were discussed. The study results indicate that the Pr^{3+}-doped oxide silicate GCs is a kind of potential phosphor.

Keywords: Pr^{3+}; X-ray diffraction; β-$BaSiO_3$ nanocrystals; phosphor

1. Introduction

For the past decades, a large amount of luminescence research has focused mainly on two aspects. One is crystal matrix [1,2] and the other is glass matrix [3,4]. But the difficulty of shaping and fibre forming of crystal and the weak luminescence properties of glass limited their further application for the optical devices. So glass ceramic (GC), as the glass and crystal composites, has attracted strong interests for their excellent luminescence properties, high uniformity and stability [5,6]. They combined the advantages of a crystalline host for *rare earth* dopants and exceptionally good luminous efficiencies, high brightness levels, transparency and glasses' ease of mass production. In GC systems, silicate GC system is one of the best choices [7,8]. They have good thermal stability and physicochemical property and they are not affected by moisture, temperature fluctuations or any sudden environmental changes. Because of the above advantages, silicate GCs comprising nanoparticles embedded in an oxide glassy matrix show promising applications in fibre amplifiers, lasers, fluorescent devices and white light emitting diode (LED).

Many presently used rare earth doped phosphors are not suitable for the excitation of InGaN-based LED chips because they cannot be excited efficiently by presently used LED chips (near ultraviolet to blue region), which results in low luminescence efficiency.

*Corresponding author. Email: sxucjlu@hotmail.com

ISSN 1745–8080 print/ISSN 1745–8099 online

DOI: 10.1080/17458080903383308
http://www.informaworld.com

Since the phosphor of Pr^{3+} emits green and red fluorescence and can be excited efficiently by 440 nm, Pr^{3+}-doped materials were studied widely [9–13]. It is also reported that the GC phosphor has various advantages over the powder phosphors for LEDs [14]. However, there are little reports describing the properties of Pr^{3+}-doped GCs phosphor and no reports describing the properties of Pr^{3+}-doped $BaO–SiO_2$ oxide GC phosphor. In this work, Pr^{3+}-doped oxide GC phosphor containing β-$BaSiO_3$ nanocrystals has been successfully prepared and its luminescence has also been investigated.

2. Experimental

Pr^{3+}-doped $60SiO_2–40BaO–0.1Pr_2O_3$ (mol %) glass was prepared using the conventional melting in silica crucible at 1600°C for about 40 min and quenching method described in Ref. [15]. The quenched sample was annealed at a temperature 450°C for 2 h and cooled slowly to release the thermal stress associated with these glasses during the quenching process. Differential thermal analysis (DTA) was carried out on Netzsch DTA404PC in an ambient atmosphere with heating rate at 10°C min^{-1} in order to determine the glass transition temperature (T_g) and the crystallised peak temperature (T_c). According to the DTA curves the glass samples were heat-treated to different temperatures at a rate of 10 K min^{-1}, held for 2 h and then cooled to room temperature naturally to obtain the transparent GC. X-ray diffraction (XRD) measurements were performed in a X′TRA diffractometer with Cu–K_α radiation at 4°C min^{-1} scanning rate. The microstructures of the samples were studied using a transmission electron microscope (TEM, H-7650). The Raman spectrum was recorded on a SL Raman spectrophotometer P1-532 HR within the range 100–1200 cm^{-1}. The excitation and the emission luminescence spectra were measured with a Jobin-Yvon Frolog3 fluorescence spectrophotometer. In order to compare the luminescence intensity of Pr^{3+} in different samples as accurately as we can, the position and the power (100 mW) of a pumping beam of 440 nm and the width (1 mm) of the slit to collect the luminescence signals were set at the same place in the experimental setup. All the measurements were taken at room temperature.

3. Results and discussion

Figure 1 shows the DTA curve of the $60SiO_2–40BaO–0.1Pr_2O_3$ oxide glass, where $T_g = 590$°C and $T_c = 860$°C stand for the glass transition temperature and crystallisation peak temperatures, respectively. Therefore, crystallisation conditions 800°C, 820°C and 840°C for 2 h were selected to form transparent GCs, and named as GC-800, GC-820 and GC-840, respectively.

The XRD patterns of the samples are presented in Figure 2a. The precursor glass is completely amorphous with no obvious diffraction peaks. After heat treatment, XRD patterns show intense diffraction peaks, which are easily assigned to the β-$BaSiO_3$ crystal (JCPDS Nos. 26-1402). With the increase in heat treatment temperature, the diffraction peaks become sharper, which indicates an increase in crystal sizes. From the peak width of XRD pattern, the crystal size of β-$BaSiO_3$ crystals in the glass matrix can be estimated by using Scherrer's equation:

$$D = K\lambda/\beta\cos\theta, \tag{1}$$

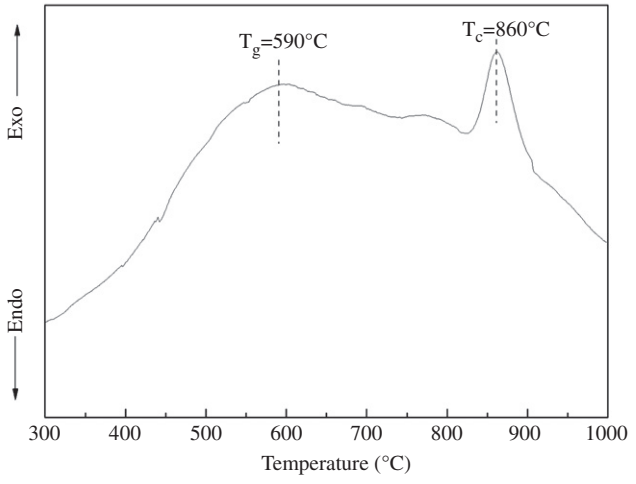

Figure 1. DTA curve of the $60SiO_2$–$40BaO$–$0.1Pr_2O_3$ oxide glass.

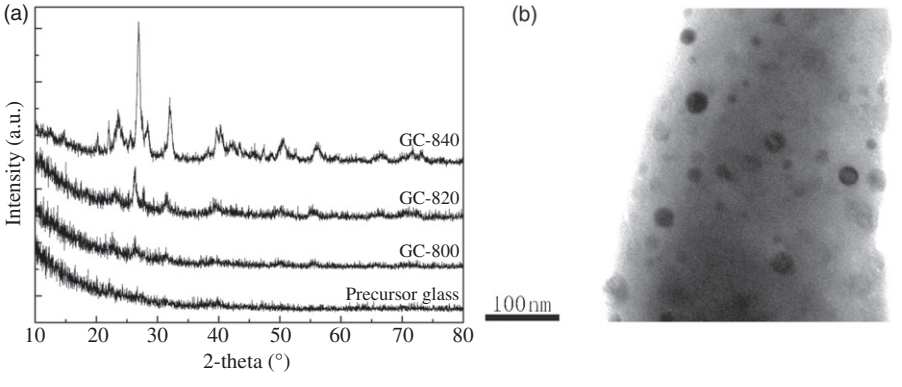

Figure 2. (a) XRD patterns of the precursor glass and GCs and (b) TEM image of the GC-840.

where D is the crystal size at the vertical direction of (hkl), λ is the wavelength of X-ray, θ is the angle of diffraction, β is the corrected full-width at half maximum (FWHM) of the diffraction peak and the constant K is determined by β and the instrument. The calculated size of the average of β-$BaSiO_3$ nanocrystals were about 8, 15 and 24 nm for GC-800, GC-820 and GC-840, respectively. The TEM image of the GC-840 (Figure 2b) demonstrates that nanoparticles sized about 24 nm are distributed homogeneously in the glass matrix. Due to much smaller size of precipitated β-$BaSiO_3$ nanocrystals than wavelength of visible light the Pr^{3+}-doped GCs remain transparent.

Figure 3 shows the room temperature Raman spectrum of precursor glass, GC-800, GC-820 and GC-840. In silicate glasses [16], the bands around 1060, 950 and 585 cm^{-1} are assigned to stretching vibrations of Si–O–Si, $^{-}$O–Si–O^{-} and Si–O^{-} groups, respectively. From Figure 3 scattering peaks at 1068, 940 and 578 cm^{-1} in precursor glass were found, and with increasing heat treatment temperature, the 1068, 940 and 578 cm^{-1} scattering

peaks move to long wavelength at 1062, 928 and 546 cm^{-1} in GC-840. After heat treatment the bands get structurised and new bands at 247, 284, 381, 491, 525 and 622 cm^{-1} were found. Several weak intensity bands at 311, 473, 738, 962 and 1024 cm^{-1} were also observed. All the sharp bands exactly match the bending vibrations peaks of Si–O–Si of $[SiO_3]^{2-}$ in crystals [17] which also indicate that the β-$BaSiO_3$ nanocrystals are formed in Pr^{3+}-doped GCs.

Figure 4 presents the excitation spectrum of GC-840, which was measured by monitoring an intense emission at 605 nm. There are three obvious excitation peaks from

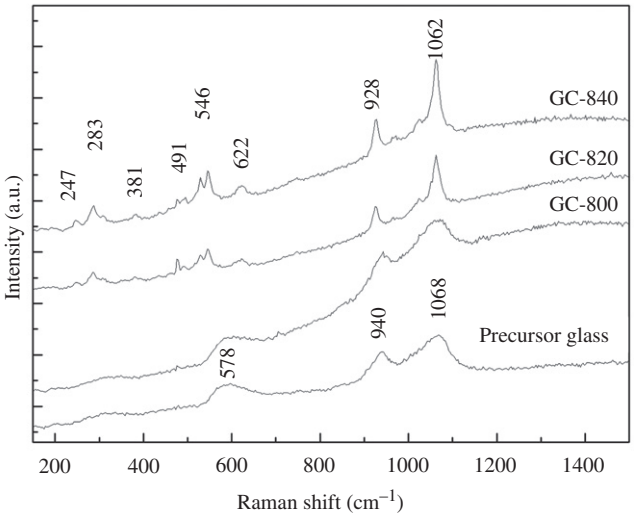

Figure 3. Room temperature Raman spectrum of precursor glass, GC-800, GC-820 and GC-840.

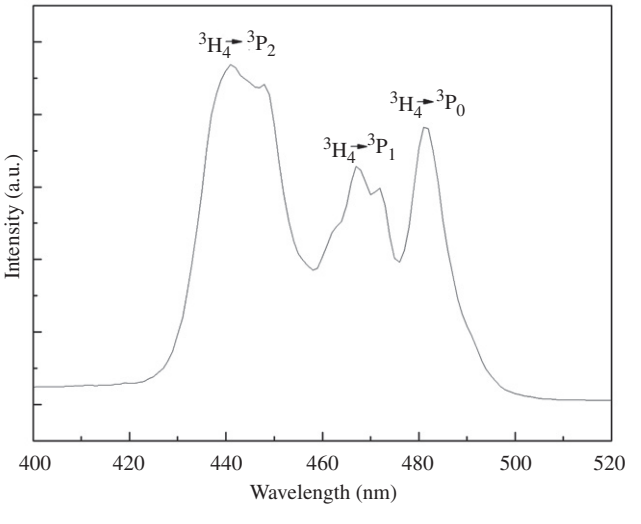

Figure 4. Excitation spectrum of GC-840 monitoring an intense emission at 605 nm.

the excitation spectrum, and these are assigned to the electronic transitions with the ground level $^3H_4$ to higher energy levels $^3H_4 \rightarrow {}^3P_2$ (440 nm), $^3H_4 \rightarrow {}^3P_1$ (467 nm) and $^3H_4 \rightarrow {}^3P_0$ (483 nm) of Pr^{3+}. From these excitation transitions, the 440 nm wavelength has been selected for the measurement of emission spectrum (because the intensity of 440 nm excitation bands is the strongest of the three).

The room temperature emission spectrum in the range 450–750 nm for Pr^{3+} ions in precursor glass and GCs under 440 nm excitation is shown in Figure 5. Two strong emission bands at 483 nm($^3P_0 \rightarrow {}^3H_4$), 605 nm($^3P_0 \rightarrow {}^3H_6$) and five more weak emission bands at 525 nm($^3P_1 \rightarrow {}^3H_5$), 538 nm($^3P_0 \rightarrow {}^3H_5$), 644 nm($^3P_0 \rightarrow {}^3F_2$), 698 nm($^3P_0 \rightarrow {}^3F_3$) and 727 nm($^3P_0 \rightarrow {}^3F_4$) are observed from these spectra for both glass and GC. Compared with the precursor glass, significant enhancement of luminescence was observed in the Pr^{3+} doped GCs. The reasons were as follows: on the one hand, the doped Pr^{3+}-ions should be incorporated into the fixed crystalline site positions [18]. Structurally, glass is a continuous random network lacking both symmetry and periodicity. In the case of glasses, the coordination of the rare earth ions becomes more delocalised. As a consequence the oscillator strengths also are more dispersed. As shown in Figure 2, β-$BaSiO_3$ crystal is formed after heat treatment and with the increase in heat treatment temperature crystalline phase increased. Therefore the emission luminescence intensity of the GCs increased significantly with increasing heat treatment temperature. On the other hand, intensity of luminescence was very sensitive to the multi-phonon relaxation rate of the rare earth ions, which greatly depends on the phonon energy of their matrix. The larger the phonon energy and (or) the electron–phonon coupling strength, the larger the decay rate. That is to say, a decrease in the phonon energy and/or electron–phonon coupling strength increases the lifetime and quantum efficiency of excited levels, and consequently increases the emission intensity of the luminescence [19]. Based on the results of Raman analysis as shown in Figure 3, the stretching vibrations Si–O^- (578 cm^{-1}), $^-$O–Si–O^- (940 cm^{-1}) and Si–O–Si (1068 cm^{-1}) in precursor silicate oxide glass are moved to lower energy Si–O^- (546 cm^{-1}), $^-$O–Si–O^- (928 cm^{-1}) and Si–O–Si (1062 cm^{-1}) in GC-840 GCs. It can be concluded that

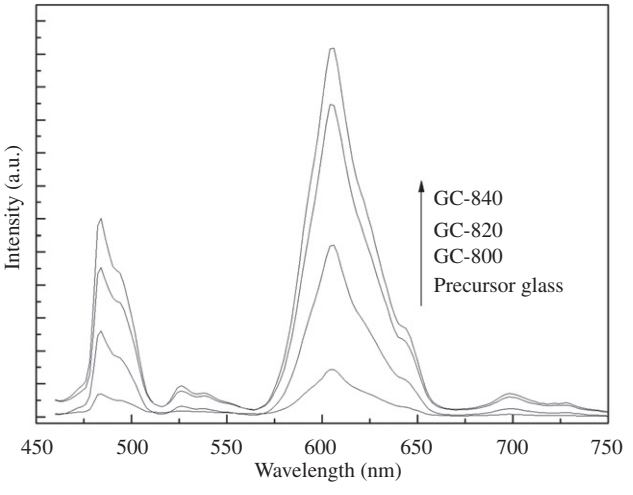

Figure 5. Emission spectrum for Pr^{3+} ions in precursor glass and GCs under 440 nm excitation.

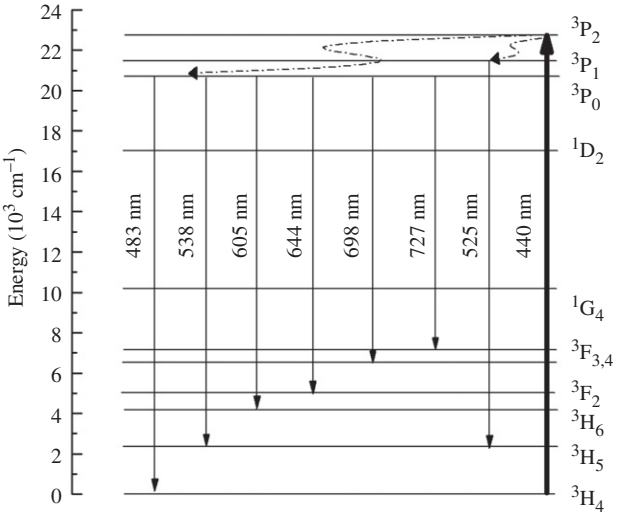

Figure 6. Simple energy level diagram of Pr^{3+} ions and the possible conversion mechanism.

the maximum phonon energy of GCs decrease with increasing heat treatment temperature. At the same time, new lower energy stretching vibrations at 247, 284, 381, 491, 525 and 622 cm^{-1} owing to Si–O–Si of $[SiO_3]^{2-}$ of β-$BaSiO_3$ nanocrystals were found in GCs. The above two reasons lead to a decrease in the non-radiative decay rate. Thus on comparison with the precursor glass, the emission intensity of the GCs is more.

Figure 6 describes the energy level scheme for the emission process observed for the Pr^{3+} ions doped GCs with 440 nm excitation wavelength. Firstly, the $^3H_4$ level of Pr^{3+} ions is directly excited with 440 nm light by means of ground state absorption (GSA) to $^3P_2$ level. Secondly, the populated $^3P_2$ level of Pr^{3+} ions then decays non-radiatively to the lower energy states $^3P_1$ and $^3P_0$. Then the state $^3P_1$ transmits to the state $^3H_5$ producing the 528 green emissions. The populated $^3P_0$ excited state transmits to the lower energy states $^3F_4$, $^3F_3$, $^3F_2$, $^3H_6$, $^3H_5$ and the ground state $^3H_4$ giving the 727 nm, 698 nm, 644 nm, 605 nm red luminescence, 538 nm orange luminescence and 483 blue luminescence.

4. Conclusions

In conclusion, a novel Pr^{3+}-doped oxide GC containing β-$BaSiO_3$ nanocrystals has been prepared. Intense blue and red emissions centred at 483 and 605 nm, corresponding to the transitions $^3P_0 \rightarrow {}^3H_4$ and $^3P_0 \rightarrow {}^3H_6$ of Pr^{3+}, respectively, were observed for at room temperature excited at 440 nm. Compared with the precursor glass, significant enhancement of luminescence was observed in GCs. The possible reason was that crystallisation plays an important role. On the other hand, the decrease in the maximum phonon energy and the appearance of some new lower energy phonons of β-$BaSiO_3$ nanocrystals in GC reduce the non-radiative decay rate and also enhance emission intensity. Due to its strong emission luminescence, the novel Pr^{3+}-doped oxide GC may be a promising phosphor.

Acknowledgements

This work was supported by the National Natural Science Foundation of China (60508014, 50772102 and 60878024), Program for New Century Excellent Talents in University (Grant No. NCET-07-0786), the Science Technology Project of Zhejiang Province (2008C21162) and the Nature Science Foundation of Zhejiang Province (Grant No R406007).

References

[1] M. Maqbool and I. Ahmad, *Ultraviolet spectroscopy of Pr^{3+} and its use in making ultraviolet filters*, Curr. Appl. Phys. 9 (2009), pp. 234–237.
[2] S. Lange, I. Sildos, M. Hartmanova, J. Aarik, and V. Kiisk, *Luminescence properties of Sm^{3+}-doped polycrystalline ZrO_2*, J. Non-Crystalline Solids 354 (2008), pp. 4380–4382.
[3] B.V. Padlyak, W. Ryba-Romanowski, and R. Lisiecki, *Optical spectroscopy and local structure of Er^{3+} luminescence centres in CaO-Ga_2O_3-GeO_2 glasses*, J. Non-Crystalline Solids 354 (2008), pp. 4249–4255.
[4] S. Xu, W. Wang, S. Zhu, B. Zhu, and J. Qiu, *Highly efficient red, green and blue upconversion luminescence of Eu^{3+}/Tb^{3+}-codoped silicate by femtosecond laser irradiation*, Chem. Phys. Lett. 442 (2007), pp. 492–495.
[5] Q. Luo, X. Qiao, X. Fan, S. Liu, H. Yang, and X. Zhang, *Reduction and luminescence of europium ions in glass ceramics containing SrF_2 nanocrystals*, J. Non-Crystalline Solids 354 (2008), pp. 4691–4694.
[6] B. Yan and J. Wu, *Facile mixed-solvent-thermal synthesis and characterisation of LaF_3: Eu^{3+}/Tb^{3+} monodisperse nanoparticles*, J. Exp. Nanosci. 4 (2009), pp. 1–7.
[7] V. Ranganathan and L. Klein, *Sol–gel synthesis of erbium-doped yttrium silicate glass–ceramics*, J. Non-Crystalline Solid. 354 (2008), pp. 3567–3571.
[8] S. Zhou, N. Jiang, B. Zhu, H. Yang, S. Ye, G. Lakshminarayana, J. Hao, and J. Qiu, *Multifunctional bismuth-doped nanoporous silica glass: From blue-green, orange, red, and white light sources to ultra-broadband infrared amplifiers*, Adv. Funct. Mater. 18 (2008), pp. 1407–1413.
[9] S. Khiari, M. Velazquez, R. Moncorgé, J.L. Doualan, P. Camy, A. Ferrier, and M. Diaf, *Red-luminescence analysis of Pr^{3+} doped fluoride crystals*, J. Alloys Compounds 451 (2008), pp. 128–131.
[10] M.A. Gusowski, G. Dominiak-Dzik, P. Solarz, R. Lisiecki, and W. Ryba-Romanowski, *Luminescence and energy transfer in K_3GdF_6: Pr^{3+}*, J. Alloys Compounds 438 (2007), pp. 72–76.
[11] X. Liu, R. Pang, Q. Li, and J. Lin, *Host-sensitized luminescence of Dy^{3+}, Pr^{3+}, Tb^{3+} in polycrystalline CaIn2O4 for field emission displays*, J. Solid State Chem. 180 (2007), pp. 1421–1430.
[12] P. Boutinaud, E. Pinel, and R. Mahiou, *The effect of calcium concentration on the photoluminescence of $CaTiO_3$: Pr^{3+} films prepared by the sol–gel method*, Opt. Mater. 30 (2008), pp. 1033–1038.
[13] Y.G. Choi, J.H. Baik, and J. Heo, *Spectroscopic properties of Pr^{3+}: $^1D_2 \rightarrow {}^1G_4$ transition in SiO_2-based glasses*, Chem. Phys. Lett. 406 (2005), pp. 436–440.
[14] A. Engel, M. Letz, T. Zachau, E. Pawlowski, K. Seneschal-Merz, and T. Korb, *Reference-based optical characterization of glass-ceramic converter for high-power white LEDs*, Proc. SPIE 6486 (2007), pp. 64860Y-1–64860Y-10.
[15] S. Xu, Z. Yang, S. Dai, G. Wang, L. Hu, and Z. Jiang, *Upconversion fluorescence spectroscopy of Er^{3+}-doped lead oxyfluoride germanate glass*, Mater. Lett. 58 (2004), pp. 1026–1029.

[16] S. Xu, Z. Yang, J. Zhang, G. Wang, S. Dai, L. Hu, and Z. Jiang, *Upconversion fluorescence spectroscopy of Er^{3+}/Yb^{3+}-codoped lead oxyfluorosilicate glass*, Chem. Phys. Lett. 385 (2004), pp. 263–267.
[17] Dan J. Durben and George H. Wolf, *High-temperature behavior of metastable $MgSiO_3$ perovskite; A Raman spectroscopic study*, Amer. Mineralogist 77 (1992), pp. 890–893.
[18] G. Lakshminarayana, H. Yang, Y. Teng, and J. Qiu, *Spectral analysis of Pr^{3+}, Sm^{3+} and Dy^{3+}-doped transparent GeO_2–BaO–TiO_2 glass ceramics*, J. Luminescence 129 (2009), pp. 59–68.
[19] J. Qiu and Z. Song, *Nanocrystals precipitation and up-conversion luminescence in Yb^{3+}-Tm^{3+} co-doped oxyfluoride glasses*, J. Rare Earths 26 (2008), pp. 919–923.